American Mineralogist, Volume 77, pages 399–406, 1992

Crystal chemistry and symmetry of a birefringent tetragonal pyralspite$_{75}$-grandite$_{25}$ garnet

Dana T. Griffen
Department of Geology, Brigham Young University, Provo, Utah 84602, U.S.A.
Dorian M. Hatch
Department of Physics and Astronomy, Brigham Young University, Provo, Utah 84602, U.S.A.
William Revell Phillips
Department of Geology, Brigham Young University, Provo, Utah 84602, U.S.A.
Seyfi Kulaksiz
Minerals Engineering Department, Hacettepe University, Ankara, Turkey

Abstract

The crystal chemistry of a natural, birefringent garnet of composition $(Fe_{1.88}Ca_{0.75}Mg_{0.24}Mn_{0.10})_{\Sigma=2.97}(Al_{1.96}Fe_{0.03}Ti_{0.01})_{\Sigma=2.00}Si_{3.01}O_{12}$ (approximately pyralspite$_{75}$-grandite$_{25}$), produced by subduction-zone metamorphism, has been investigated by single-crystal X-ray diffraction, electron microprobe analysis, Mössbauer spectroscopy, and Fourier-transform infrared spectroscopy. By FTIR the garnet is apparently indistinguishable from synthetic garnets of similar compositions and is anhydrous. The crystal structure has been refined in space group $I4_1/acd$, using 592 unique, observed reflections measured with an automated four-circle X-ray diffractometer. Dimensions of the tetragonal unit cell are $a = 11.6207(7)$, $c = 11.6230(8)$ Å. The final conventional residuals are $R = 0.033$ and $R_w = 0.024$. X-ray site refinement indicates a slight difference in electron density at the two unique X sites, and this is apparently the cause of birefringence (~0.001). It is proposed that the difference in electron density arises from slight ordering between the pyralspite X components (Fe^{2+}, Mg, and Mn) and the grandite X component (Ca). The high pressure of the geologic environment evidently favored substantial solid solution between pyralspite and grandite end-members, whereas comparatively low temperatures prevented complete disorder.

A group theoretical analysis based on the Landau formalism and including the theory of induced representations shows that the observed space group could have arisen by phase transformation from a parent cubic garnet (space group $Ia\bar{3}d$), driven by a single order parameter in each case. Such transitions may occur (1) by the T_{2g} irreducible representation (IR), leading to possible space groups $R\bar{3}c$, $Fddd$, $C2/c$, or $I\bar{1}$; (2) by the T_{1g} IR, leading to possible space groups $R\bar{3}$, $I4_1/a$, $C2/c$, or $I\bar{1}$; or (3) by the E_g IR, leading to possible space groups $I4_1/acd$ or $Ibca$. The first two ordering paths (T_{2g} and T_{1g}) yield octahedral ordering; if the sizes of the octahedral cations are similar (as with Al and Fe^{3+} in grandites), ordering occurs by T_{2g}, and if they are very different (as in $MgSiO_3$ and $MnSiO_3$ garnets), ordering occurs by T_{1g}. Garnets that possess cations ordered in the eightfold-coordinated sites (for example, some with both significant pyralspite and grossular components) order by E_g. Thus far, the noncubic garnets with refined crystal structures possess space groups $Fddd$ and $I\bar{1}$ (T_{2g}), $I4_1/a$ (T_{1g}), and $I4_1/acd$ (E_g).

The approach presented is based on the assumption that phase transitions may have occurred to produce garnets of noncubic symmetry. The mathematical treatment used, however, yields the same predictions about possible space groups if ordering is assumed to have arisen as a crystal-growth phenomenon rather than by phase transformation. The experimental and field evidence accumulated so far does not provide clear evidence in favor of one or the other, and it is possible that each plays a role under different circumstances.

Introduction

Among the major rock-forming silicates, garnets constitute one of the few groups that crystallize with cubic symmetry. Garnets occur in a wide variety of rocks and show great variation in chemical composition, but nearly all have symmetry described by space group $Ia\bar{3}d$. In the

0003–004X/92/0304–0399$02.00

general formula, $\{X\}_3[Y]_2(Z)_3O_{12}$ (notation of Geller, 1967), $\{X\}$ is most commonly Fe^{2+}, Mg, Mn, or Ca in eightfold coordination on the Wyckoff 24c position, $[Y]$ is most commonly Fe^{3+} or Al in octahedral coordination at the Wyckoff 16a position, and (Z) is tetrahedrally coordinated Si at the Wyckoff 24d position. Natural garnets are often divided into two groups: the pyralspites, consisting of solid solutions of pyrope ($Mg_3Al_2Si_3O_{12}$), almandine ($Fe_3Al_2Si_3O_{12}$), and spessartine ($Mn_3Al_2Si_3O_{12}$); and the grandites, solid solutions of grossular ($Ca_3Al_2Si_3O_{12}$) and andradite ($Ca_3Fe_2Si_3O_{12}$). Garnets intermediate in composition between the pyralspites and the grandites are much less common than those within the two groups, although this seems to reflect the fact that the conditions of pressure, temperature, and composition required for their formation are rarely simultaneously attained rather than to imply a crystal-chemical limitation of the structure (Nemec, 1967).

Although nearly all garnets found in the crust of the Earth are isotropic, consistent with their cubic symmetry, some are not. Optically anisotropic members of the grossular-andradite solid-solution series exist, and crystal-structure refinements of five of them (Takéuchi et al., 1982; Allen and Buseck, 1988; Kingma and Downs, 1989) have shown that they crystallize in space groups *Fddd* or $I\bar{1}$. Other space groups are possible (Hatch and Griffen, 1989) but have not yet been observed. In each case, the optical (and thus structural) anisotropy has been caused by ordering of the $[Y]$ cations, Fe^{3+} and Al. [The garnet of Allen and Buseck (1988) has nearly as much almandine component as andradite component, as well as a small amount of OH; it shows ordering of Ca and Fe^{2+} on the $\{X\}$ sites and a noncubic distribution of OH groups, in addition to ordering at the $[Y]$ sites.]

In this paper we report the crystal chemistry of a natural anisotropic garnet intermediate in composition between the pyralspite and the grandite groups. Anisotropic garnets in this composition range have not previously been reported. There has been one study of a pyrope sample containing 10 mol% grossular component (Dempsey, 1980) that showed diffraction maxima on precession photographs that violated space group $Ia\bar{3}d$, but the probable space group was deduced as $I2_13$ and the garnet was not anisotropic. Additionally, the average, cubic structure of a natural birefringent spessartine sample was refined by Smyth et al. (1990), but the true structure was not.

The garnet reported here came from a rock sample designated as T-KAY-K-1 (Kulaksiz and Phillips, 1983) and will be referred to in the present paper as garnet T-KAY-K-1. The regional setting is a paleosubduction zone of mid-Cretaceous age (85.7 ± 1.67 Ma), located in northwest Turkey between Sivrihisar and Balçikhisar. The garnet occurs as highly fractured, euhedral, dodecahedron porphyroblasts in an eclogite fragment from a melange consisting mostly of low-grade marble. The rock consists largely of omphacitic pyroxene, epidote, and white mica, with less abundant garnet, rutile, and sodic amphibole.

Experimental methods

Chemical and spectroscopic methods

A room-temperature Mössbauer spectrum was obtained with the spectrometer in the Chemical Engineering Department of Brigham Young University. Velocities were varied between +4 and −4 mm/s, with metallic Fe as standard.

Chemical analyses were carried out using the Cameca electron microprobe at the Department of Geology and Geophysics of the University of Utah, at an operating voltage of 15 kV and beam current of 15 nA. Specimens analyzed consisted of polished fragments from several crystals. Well-characterized silicates and oxides were chosen as standards. Data were obtained using wavelength-dispersive spectrometers, and an energy-dispersive spectrometer was used simultaneously to monitor the analysis of each spot to ensure that all elements present above EDS detection limits were accounted for. Data reduction was carried out on-line. Analyses were performed for Si, Ti, Al, Fe, Mg, Mn, Ca, K, Na, and F; the latter three were not detected.

A Perkin Elmer 1600 series FTIR was used to obtain an infrared spectrum from a KBr pellet containing 0.25 wt% garnet. The spectrum is similar to those for synthetic almandine-grossular and almandine-pyrope garnets (Geiger et al., 1989), with bands A through I prominent (Moore et al., 1971). The spectrum showed the mineral to be anhydrous.

The garnet is weakly birefringent (biref. ≈ 0.001) with mean index of refraction 1.797 ± 0.002, measured by standard oil-immersion techniques.

Crystal structure refinement

Long-exposure precession photographs were taken of a small euhedral crystal that displayed nonuniform extinction, and no indications of twinning, noncubic lattice parameters, or reflections violating space group $Ia\bar{3}d$ were observed. A birefringent fragment with uniform extinction, approximately cubic in shape and 0.08 mm on each side, was then cut from a larger chip and mounted on a Nicolet R3 automated four-circle, single-crystal X-ray diffractometer equipped with a graphite monochromator and Mo$K\alpha$ radiation. Unit-cell parameters were determined by least-squares refinement of 25 reflections in the range $44° < |2\theta| < 59°$ automatically centered at both $+2\theta$ and -2θ. The unit cell is pseudocubic, but the results of the structure refinement, given below, show that the actual symmetry is tetragonal. The cell parameter obtained by assuming cubic symmetry is $a = 11.6215(4)$ Å.

A total of 4988 reflections were measured in the θ-2θ mode from half of the Ewald sphere out to $\sin\theta/\lambda = 0.70$. Scan speeds were automatically varied from 3.0 to 29.3° 2θ/min depending on diffracted intensity. Three standards were monitored once in every 100 reflections, and the observed intensities were corrected according to variations in the intensities of the standards. Lorentz and

polarization corrections were applied, as well as an empirical absorption correction ($\mu \approx 59$ cm^{-1}) based on ψ scans (North et al., 1968) and an isotropic extinction correction.

As a first step in determining the crystal structure, the data were refined in the average (cubic) space group $Ia\bar{3}d$. Of the 4988 intensities measured, 807 were rejected as unobserved (zero or negative intensities), and the remaining 4181 were reduced to a symmetry-merged set of 201 unique reflections, of which 190 had $I > 3\sigma(I)$ and were used in the refinement. Starting positional parameters for the O atom (the only atom not on a special position) were approximated from the regression equations of Novak and Gibbs (1971). Atomic scattering factors were taken from Cromer and Mann (1968) and anomalous-dispersion factors from Cromer and Liberman (1970). Data processing and refinement were carried out with the program package SHELXTL (Sheldrick, 1983).

By varying the positional parameters for O, isotropic temperature factors for all atoms, and site-occupancy factors for the $\{X\}$ and $[Y]$ cations, refinement converged rapidly to $R = 0.06$. Adoption of anisotropic temperature-factor coefficients for all atoms and of a weighting scheme [$w = 1/\sigma^2(F)$] led to conventional residuals of $R = 0.045$ and $R_w = 0.028$. The final refined O position in this average space group has $x = 0.0347(2)$, $y = 0.0476(2)$, $z = 0.6525(2)$; based on modeled occupancy by Ca and Al, the site occupancy factors of the $\{X\}$ and $[Y]$ sites are 1.168(4) and 0.991(8), respectively.

In an attempt to determine the true symmetry, the structure was refined in space group $I\bar{1}$ and a difference-Fourier map was calculated with Ca in the six symmetrically unique X sites, Al in the eight Y sites, and Si in the six Z sites. The only significant peaks on the difference map were at the X positions and ranged from 5.5 to 5.9 e/Å^3 in height; they were not different enough to provide a clear indication of the true symmetry. Metrically, however, the triclinic unit cell, in the same orientation as the cubic cell used above, had dimensions $a = 11.622(1)$, $b = 11.625(1)$, and $c = 11.622(1)$ with interaxial angles all statistically 90°; this suggested the possibility of a tetragonal unit cell with basis vectors $\mathbf{a}_t \approx \mathbf{c}_c$, $\mathbf{b}_t \approx \mathbf{a}_c$, $\mathbf{c}_t \approx \mathbf{b}_c$, where subscripts t and c refer to tetragonal and cubic, respectively. Possible tetragonal space groups that are subgroups of $Ia\bar{3}d$, and thus would allow the garnet structure to be maintained, are $I4_1/acd$ and $I4_1/a$. Refinement in space group $I4_1/acd$ was attempted.

The refined unit-cell dimensions, assuming tetragonal symmetry and using the same 25 reflections obtained for the cubic-cell refinement, are $a = 11.6207(7)$ and $c = 11.6230(8)$. Merging of the original 4988 reflections in Laue group $4/mmm$ resulted in 592 symmetry-independent reflections, of which the 428 that had $I > 3\sigma(I)$ were used in the refinement. Starting values for variable positional parameters were determined by adding small, random amounts to the corresponding values obtained in one of the intermediate stages of the cubic refinement. The initial four cycles of unweighted least-squares refinement, in which positional and isotropic thermal parameters but not site occupancy factors were varied, converged to $R = 0.06$. The introduction of anisotropic temperature-factor coefficients, variable site-occupancy factors for the two unique X sites and the single unique Y site in this space group, and a weighting scheme [$w = 1/\sigma^2(F)$] resulted in final residuals of $R = 0.033$ and $R_w = 0.024$. Observed and calculated structure amplitudes for the tetragonal refinement are given in Table 1.[1]

Results and discussion

Chemical relations

Results of the microprobe analysis are presented in Table 2, with end-member concentrations calculated by the method of Rickwood (1968). FeO obtained by microprobe was converted to FeO + Fe_2O_3 by assuming that the deficiency of Al + Ti available for the Y site is made up by Fe^{3+}. Minor chemical heterogeneity was noted in the analyses from spot to spot and from grain to grain. At the spots analyzed, Mn varies from 0.89 to 2.17 wt%, corresponding to 0.07 to 0.15 atoms per 12 O atoms, and Mg varies from 0.05 to 0.18 wt%, corresponding to 0.21 to 0.28 atoms per 12 O atoms. Moreover, Mn and Mg vary antipathetically, whereas concentrations of all other elements remain virtually constant, indicating mutual substitution of spessartine and pyrope components. Given the low concentrations of both components, the compositional variations do not significantly affect the results of the crystal-structure refinement.

The Mössbauer spectrum (Fig. 1) was fitted with four Lorentzian peaks constrained to be equal in width and intensity as doublets. The result yielded one Fe^{2+} doublet with an isomer shift of 1.31 mm/s and quadrupole splitting of 3.56 mm/s and one Fe^{3+} doublet with an isomer shift of 0.37 mm/s and quadrupole splitting of 0.44 mm/s. The χ^2 value for the fit is 1.095. Peak areas indicate that 94% of Fe_{tot} is Fe^{2+} and 6% is Fe^{3+}, but the spectrum exhibits substantial scatter in the Fe^{3+} region and considerable error in these percentages is suspected (see, for example, Dyar, 1984, concerning errors in peak areas). Further, the X-ray site refinement discussed below does not support this much Fe^{3+}. We have taken the microprobe results reported above to be a more accurate approximation of Fe^{3+} concentration, but the Mössbauer spectrum does confirm the presence of minor trivalent Fe.

The site-occupancy factors for the two unique X sites refined to 1.182 and 1.171, corresponding on (weighted) average to an atom with 17.8% more scattering power than Ca (the model atom used in the refinement), in good

[1] Copies of Tables 1, 4, 10, and 11 may be ordered as Document AM-92-493 from the Business Office, Mineralogical Society of America, 1130 Seventeenth Street NW, Suite 330, Washington, DC 20036, U.S.A. Please remit $5.00 in advance for the microfiche.

TABLE 2. Chemical composition of garnet T-KAY-K-1

	Ox. wt%		Cations*
SiO_2	37.86		3.01
TiO_2	0.11		0.01
Al_2O_3	20.93		1.96
Fe_2O_3**		0.51	0.03
FeO**	28.74	28.28	1.88
MnO	1.53		0.10
MgO	2.02		0.24
CaO	8.84		0.75
	100.03		7.98

$(Fe_{1.86}Ca_{0.75}Mg_{0.24}Mn_{0.10})_{\Sigma=2.97}(Al_{1.96}Fe_{0.03}Ti_{0.01})_{\Sigma=2.00}Si_{3.01}O_{12}$
$(alm_{62.7}prp_{8.0}sps_{3.4})(grs_{23.5}adr_{1.3})(sch_{0.2})$† ≈ $pyralspite_{75}$-$grandite_{25}$

* Normalized to 12 O atoms.
** See text for discussion of Fe^{2+}/Fe^{3+}.
† See Kretz (1983) for abbreviations of components; sch = schorlamite.

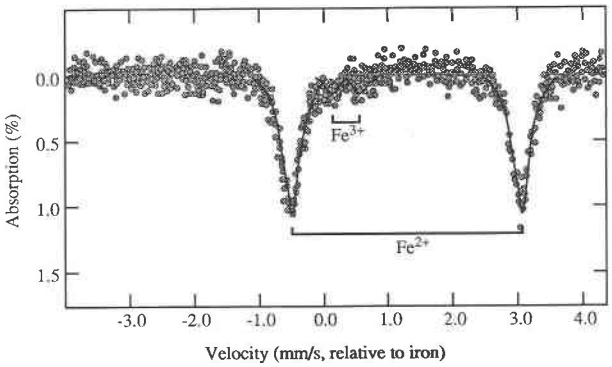

Fig. 1. The Mössbauer spectrum of garnet T-KAY-K-1.

agreement with the chemical formula $\{X\} = Fe_{1.88}Ca_{0.75}Mg_{0.24}Mn_{0.10}$ (16.6% more scattering power than Ca). The occupancy factor for the Y site refined to a value corresponding to occupancy by Al within a standard deviation, about 1.8% less than implied by the formula $[Y] = Al_{1.96}Fe_{0.03}Ti_{0.01}$.

Crystal structure

Because of the somewhat unusual composition of this garnet (approximately $pyralspite_{0.75}$-$grandite_{0.25}$) and the fact that it deviates so little from cubic symmetry, the bond lengths and angles for the average structure are given in Table 3 and the anisotropic temperature-factor coefficients are given in Table 4[1] to facilitate comparison with other garnet structures refined in space group $Ia\bar{3}d$.

Owing to the pseudosymmetry of garnet T-KAY-K-1, each of the several possibilities for the correct space group may yield apparently acceptable refinement results. Anisotropic garnets of quite different compositions from this one have been refined in space groups $I\bar{1}$ (Takéuchi et al., 1982; Allen and Buseck, 1988; Kingma and Downs, 1989), *Fddd* (Takéuchi et al., 1982), and $I4_1/a$ (Prewitt and Sleight, 1969; Fujino et al., 1986; Angel et al., 1989), and other space groups are possible (see Hatch and Griffen, 1989). Although R_{int} values obtained on averaging equivalent reflections sometimes clearly indicate the correct Laue group, the values obtained for $m3m$, $4/mmm$, $4/m$, and mmm were too close to be conclusive—0.024, 0.023, 0.021, and 0.021, respectively. During the course of this study, structure refinements were attempted in space groups $I4_1/acd$, $I4_1/a$, *Fddd*, $I\bar{1}$, and *Ibca* (the last is a subgroup of $I4_1/acd$), and the generalized weighted R factor, R_g, (Hamilton, 1965) was used to test each refinement against the cubic model. Table 5 shows the results of these tests. Note that tests to determine if a given model is significantly better than the cubic model are shown only for $I4_1/acd$ and *Ibca* because the other three refinements yielded higher R_g values than did the cubic refinement and thus cannot be preferred. The clear choice for the correct space group is $I4_1/acd$. Final positional parameters, site-occupancy factors, equivalent isotropic temperature factors, and anisotropic temperature-factor coefficients for refinement in space group $I4_1/acd$ are displayed in Table 6, and selected interatomic distances and angles are in Table 7.

TABLE 3. Selected interatomic distances (Å) and angles (°) from refinement of garnet T-KAY-K-1 in the averge space group, $Ia\bar{3}d$

Si-O	1.640(2)		
2 O1-O2	2.521(4)	2 O1-Si-O2	100.5(1)
4 O1-O3	2.752(3)	4 O1-Si-O3	114.1(1)
Y-O	1.902(2)		
6 O1-O4	2.673(3)	6 O1-*Y*-O4	89.3(1)
6 O1-O5	2.706(3)	6 O1-*Y*-O5	90.7(1)
4*X*1-O4	2.244(2)		
4*X*2-O4	2.407(2)		
	2.326		
2 O1-O2	2.519(3)	2 O1-*X*2-O2	68.3(1)
4 O1-O4	2.674(3)	4 O1-*X*2-O4	70.1(1)
4 O4-O6	2.818(4)	4 O4-*X*2-O6	74.5(1)
2 O4-O7	2.826(4)	2 O4-*X*2-O7	71.9(1)
4 O1-O7	3.367(4)	4 O1-*X*2-O7	92.7(1)
2 O8-O7	3.948(4)	2 O8-*X*2-O8	110.2(1)

Note: Numbers in parentheses are estimated standard deviations and refer to last decimal place. This convention applies to subsequent tables.

Why is garnet T-KAY-K-1 noncubic? The anisotropic grandites thus far submitted to crystal-structure refinement (Takéuchi et al., 1982; Kingma and Downs, 1989) have shown ordering of Al and Fe^{3+} at the octahedral sites (Wyckoff symbol 16a in the average cubic space group). A chemically more complicated garnet of composition $Gro_{90}And_6Alm_4$ (Allen and Buseck, 1988) with a significant H_2O content shows ordering of Al and Fe^{3+} at the octahedral sites, ordering of Ca and Fe^{2+} at the dodecahedral sites (cubic 24c positions), and a noncubic distribution of OH ions.

Table 8 shows a comparison of the crystallographic positions occupied in cubic garnets and the analogous positions in space group $I4_1/acd$, and Figure 2 shows a slab of the garnet structure with the unique cation sites indicated. Given that there is no evidence of anionic substitution in garnet T-KAY-K-1, that the tetrahedral sites are completely filled with Si, and that there is only one symmetrically unique kind of octahedral site, the X sites

TABLE 5. Significance tests on refinements

H_0: The $Ia\bar{3}d$ model ($R_g = 0.0205$) is the better of the two in question

1. $I4_1/a$
   $R_g = 0.0210$ $R_g(Ia\bar{3}d) < R_g(I4_1/a)$, $\therefore$ H_0 is accepted
2. $Fddd$
   $R_g = 0.0220$ $R_g(Ia\bar{3}d) < R_g(Fddd)$, $\therefore$ H_0 is accepted
3. $I\bar{1}$
   $R_g = 0.0314$ $R_g(Ia\bar{3}d) < R_g(I\bar{1})$, $\therefore$ H_0 is accepted
4. $Ibca$
   $R_g = 0.0190$ $R' = 0.0205/0.0190 = 1.079$ $\Re_{83,594,0.005} = 1.094$
   $\Re > R'$, $\therefore$ H_0 is accepted at the 0.005 significance level
5. $I4_1/acd$
   $R_g = 0.0185$ $R' = 0.0205/0.0185 = 1.108$ $\Re_{33,375,0.005} = 1.076$
   $\Re < R'$, $\therefore$ H_0 is rejected at the 0.005 significance level, $I4_1/acd$ is the better model

turn out to be the only possible locations on which ordering could occur. Table 6 shows that the electron density at the $X1$ sites is slightly greater than that at $X2$, whereas Table 7 shows that $X1$ is the slightly smaller of the two sites. From Table 2 and the ionic radii of Shannon (1976), it can be determined (1) that the eightfold-coordinated ionic radius of the mean pyralspite X component is 0.92 Å and that the radius of $^{[8]}Ca^{2+}$, the only grandite X cation, is 1.12 Å and (2) that the average weighted atomic number of the pyralspite X component is 24.4, whereas that of Ca is 20. Although both the differences between the mean bond lengths of the two X sites and the difference between the electron densities at these sites are very small (<1 esd for the bond lengths and ~2 combined esd for occupancy factors) and might be considered trivial considered alone, they are consistent with slight ordering of (Fe,Mg,Mn) into $X1$ and Ca into $X2$ of the tetragonal garnet.

SYMMETRY ANALYSIS

Hatch and Griffen (1989) have considered noncubic garnets in general, and birefringent grandites in particular, within the framework of the Landau theory of phase transitions (Landau, 1937a, 1937b, with extensions by Birman, 1966; Goldrich and Birman, 1968; Jaric and Birman, 1977; Hatch 1981a, 1981b; Hatch and Stokes, 1985, 1986) and the theory of induced representations (Hatch et al., 1987). On the assumption that noncubic garnets may arise by phase transformations from an initially cubic phase of space group $Ia\bar{3}d$ and that the transitions are driven by a single order parameter (not necessarily the same one in all cases), they have determined that there are three ordering routes possible: one involving an order parameter that transforms according to the T_{2g} irreducible representation (IR), one involving an order parameter that transforms according to the T_{1g} IR, and one involving an order parameter that transforms according to the

TABLE 7. Selected interatomic distances (Å) and angles (°), polyhedral volumes (Å³), quadratic elongations, and angle variances* for garnet T-KAY-K-1 refined in space group $I4_1/acd$

2 Si1-O1	1.638(2)	O1-O1	2.517(4)	O1-Si1-O1	100.4(2)
2 Si1-O3	1.642(2)	O3-O3	2.525(5)	O3-Si1-O3	100.5(2)
	1.640	4 O1-O3	2.753(3)	4 O1-Si1-O3	114.2(1)
			2.676		109.6
	V = 2.222		$\langle\lambda\rangle$ = 1.012	σ^2 = 50.02	
4 Si2-O2	1.640(2)	2 O2-O2	2.527(4)	2 O2-Si2-O2	100.8(2)
		4 O2-O2	2.750(4)	4 O2-Si2-O2	114.0(1)
			2.676		109.6
	V = 2.224		$\langle\lambda\rangle$ = 1.011	σ^2 = 46.28	
2 *Y*-O2	1.898(2)	2 O1-O2	2.671(3)	2 O1-*Y*-O2	89.3(1)
2 *Y*-O3	1.899(2)	2 O1-O2	2.703(3)	2 O1-*Y*-O2	90.7(1)
2 *Y*-O1	1.902(2)	2 O1-O3	2.673(3)	2 O1-*Y*-O3	89.4(1)
	1.900	2 O1-O3	2.701(3)	2 O1-*Y*-O3	90.6(1)
		2 O2-O3	2.672(3)	2 O2-*Y*-O3	89.5(1)
		2 O2-O3	2.698(3)	2 O2-*Y*-O3	90.5(1)
			2.686		90.0
	V = 9.136		$\langle\lambda\rangle$ = 1.000	σ^2 = 0.41	
2 *X*1-O1	2.244(2)	O1-O1	2.517(4)	O1-*X*1-O1	68.2(1)
2 *X*1-O3	2.244(2)	O3-O3	2.525(5)	O3-*X*1-O3	68.5(1)
2 *X*1-O2	2.408(2)	2 O1-O2	2.671(3)	2 O1-*X*1-O2	70.0(1)
2 *X*1-O1	2.410(2)	2 O1-O3	2.673(3)	2 O1-*X*1-O3	70.0(1)
	2.327	2 O1-O1	2.821(5)	2 O1-*X*1-O1	74.5(1)
		2 O2-O3	2.825(3)	2 O2-*X*1-O3	74.7(1)
		2 O1-O2	2.827(3)	2 O1-*X*1-O2	71.9(1)
		2 O1-O1	3.366(4)	2 O1-*X*1-O1	92.6(1)
		2 O2-O3	3.367(3)	2 O2-*X*1-O3	92.7(1)
		2 O1-O2	3.953(3)	2 O1-*X*1-O2	110.3(1)
			3.003		80.6
	V = 21.67		$\langle\lambda\rangle$ = 1.001	σ^2 = 199.41	
4 *X*2-O2	2.249(2)	2 O2-O2	2.527(4)	2 O2-*X*2-O2	68.4(1)
4 *X*2-O3	2.407(2)	4 O2-O3	2.672(3)	4 O2-*X*2-O3	70.0(1)
	2.328	2 O3-O3	2.828(5)	2 O3-*X*2-O3	72.0(1)
		4 O2-O3	2.825(3)	4 O2-*X*2-O3	74.6(1)
		4 O2-O3	3.370(3)	4 O2-*X*2-O3	92.7(1)
		2 O3-O3	3.948(5)	2 O3-*X*2-O3	110.2(1)
			3.004		80.6
	V = 21.72		$\langle\lambda\rangle$ = 1.001	σ^2 = 198.65	

* For method of calculation of quadratic elongation ($\langle\lambda\rangle$) and angle variance (σ^2), see Robinson et al. (1971). For the X sites, the mean values of the bond lengths and bond angles were used as the ideal values.

TABLE 6. Final fractional coordinates, site-occupancy factors, anisotropic temperature-factor coefficients (×10⁴), and equivalent isotropic temperature factors (×10⁴) for garnet T-KAY-K-1 refined in space group $I4_1/acd$

	x	y	z	k*	U_{11}**	U_{22}	U_{33}	U_{23}	U_{13}	U_{12}	U_{eq}
*X*1	0.1249(1)	0	¼	1.182(4)	76(4)	134(5)	130(4)	12(4)	0	0	113(2)
*X*2	0	¼	⅛	1.171(5)	128(4)	(U_{11})	68(5)	0	0	16(5)	108(3)
Y	0	0	0	1.001(5)	81(7)	84(7)	83(5)	−5(6)	−6(6)	1(6)	58(4)
Si1	0.3749(1)	0	¼		106(6)	91(7)	89(6)	−1(5)	0	0	96(4)
Si3	0	¼	⅜		86(6)	(U_{11})	111(9)	0	0	0	94(4)
O1	0.2848(2)	0.0973(2)	0.2025(2)		126(13)	126(13)	116(11)	1(11)	−20(10)	9(9)	123(7)
O2	0.0977(2)	0.2024(2)	0.2851(2)		114(13)	114(12)	133(11)	−9(10)	2(10)	10(9)	120(7)
O3	0.2024(2)	0.2847(2)	0.0976(2)		136(12)	118(12)	113(11)	1(10)	7(11)	−5(9)	122(7)

* Site occupancy. Scattering factor for Ca was used in the X site and for Al in the Y site.
** U_{ij} are coefficients in the expression $\exp[-2\pi^2(U_{11}h^2a^{*2} + U_{22}k^2b^{*2} + U_{33}l^2c^{*2} + 2U_{12}hka^*b^* + 2U_{13}hla^*c^* + 2U_{23}klb^*c^*)]$.

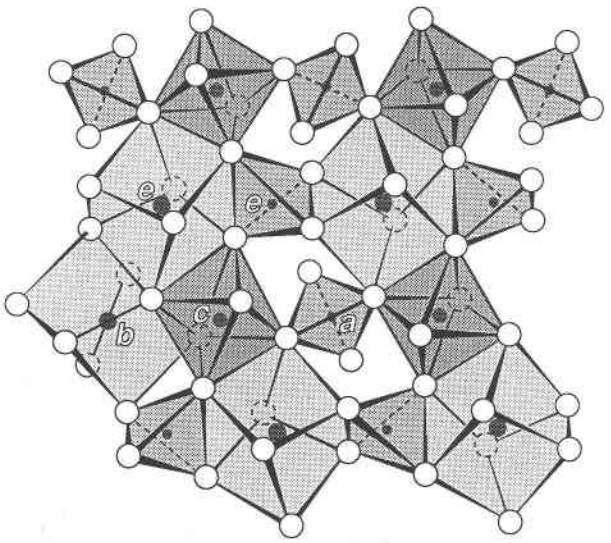

Fig. 2. A slab of the garnet structure (after Novak and Gibbs, 1971), with Wyckoff letters for the unique cations sites in space group $I4_1/acd$ indicated.

E_g IR. The T_{2g} route leads to possible space groups $R\bar{3}c$, *Fddd*, *I*2/*c*, and $I\bar{1}$; the T_{1g} route leads to possible space groups $R\bar{3}$, $I4_1/a$, *I*2/*c*, and $I\bar{1}$; and the E_g route leads to possible space groups $I4_1/acd$ and *Ibca*.

The transformation from $Ia\bar{3}d$ to $I4_1/acd$ is a proper ferroelastic transition that must be associated with the Γ point of the Brillouin zone. The space group $I4_1/acd$ is necessarily related to the parent space group by an order parameter that transforms according to the E_g IR (Γ_3^+ in the notation of Stokes and Hatch, 1988).

Table 9 gives the two space groups, and their relationships to $Ia\bar{3}d$, that may result from phase transformations that are driven by a single order parameter using the E_g IR. The η_i shown in the last column are components of the order parameter, η, in the equation $\rho(r) = \rho_0(r) + \Sigma\eta_i\phi_i(r)$. Here $\rho(r)$ is the density function that specifies the probability distribution of atomic positions in the crystal, with $\rho_0(r)$ being the density function in the parent (high-symmetry) space group. The $\phi_i(r)$ are the basis functions of a physically irreducible representation of the parent space group ($Ia\bar{3}d$ in this case), so that the order parameter components, η_i, give the contribution of each basis function to the density function. The ordering, in this case, is between the (Fe^{2+},Mg,Mn) that constitute the pyralspite *X* components and Ca, the grandite *X* component;

Table 8. Occupied sites in $Ia\bar{3}d$ and $I4_1/acd$ garnet structures

$Ia\bar{3}d$			$I4_1/acd$		
{*X*}	24c	⅛, 0, ¼	*X*1	16e	*x*, 0, ¼
			*X*2	8b	0, ¼, ⅛
[*Y*]	16a	0, 0, 0	*Y*	16c	0, 0, 0
(*Z*)	24d	⅜, 0, ¼	Si1	16e	*x*, 0, ¼
			Si2	8a	0, ¼, ⅜
O	96h	*x*, *y*, *z*	O1	32g	*x*, *y*, *z*
			O2	32g	*x*, *y*, *z*
			O3	32g	*x*, *y*, *z*

Table 9. Subgroups of $Ia\bar{3}d$ allowed by the E_g IR

Subgroup	Origin	Basis vectors	Direction of vector η
$I4_1/acd$	(0,0,0)	(1,0,0),(0,1,0),(0,0,1)	$(\eta_1,0)$
Ibca	(0,0,0)	(1,0,0),(0,1,0),(0,0,1)	(η_1,η_2)

it takes place on the 24 {*X*} sites of the cubic unit cell, thus lowering the symmetry from $Ia\bar{3}d$ to $I4_1/acd$.

In Table 10[1] the splitting of the equivalent points of the Wyckoff 24c position of $Ia\bar{3}d$ into the 8b and 16e positions of $I4_1/acd$ are listed. In Table 11[1] the two basic functions that transform according to the E_g representation (Γ_3^+) are shown. The relative degree of ordering on the 24c points of $Ia\bar{3}d$ represents the ordering of the *X* components; their positions in $Ia\bar{3}d$ are also shown. For the order parameter (η_1, 0) shown in Table 9 (that is, for space group $I4_1/acd$), only the first basis function of Table 11 contributes. Note that any individual site on an 8b Wyckoff point shows twice the ordering of an individual site on a 16e point, as required by the relative numbers of points constituting the Wyckoff positions.

From Stokes and Hatch (1988), the Γ_3^+ representation does not satisfy the Landau condition; thus the transition must be discontinuous. The free energy for Γ_3^+ is

$$\Delta F = a(\eta_1^2 + \eta_2^2) + b(\eta_1^3 - 3\eta_1\eta_2^2) + c(\eta_1^2 + \eta_2^2)^2.$$

The free energy form will yield many physical properties that undergo a change of symmetry at the transition as a result of a Γ_3^+ order parameter becoming nonzero. For example, heat capacity and enthalpy as a function of temperature can be obtained. The spontaneous strain components ($\epsilon_{11} + \epsilon_{22} - 2\epsilon_{33}$, $\sqrt{3}\epsilon_{11} - \sqrt{3}\epsilon_{22}$) also transform as the two components of Γ_3^+. Thus these strain components, denoted (Q_1,Q_2), will couple bilinearly to (η_1,η_2) in the form $\eta_1Q_1 + \eta_2Q_2$ and will also become nonzero at the transition. Because only the first component is nonzero at the transition to $I4_1/acd$, only the first component of the spontaneous strain Q_1 ($\equiv \epsilon_{11} + \epsilon_{22} - 2\epsilon_{33}$) will become nonzero.

Conclusion

On the basis of the discussion above, we interpret the anisotropy of garnet T-KAY-K-1 as due to slight ordering of the pyralspite (Fe^{2+},Mg,Mn) and grandite (Ca) *X* components on the 24c positions of the average $Ia\bar{3}d$ structure. There are, of course, small shifts in the O and Si positions relative to those positions in the average cubic structure, but we take these to be secondary consequences of *X*-site ordering, inasmuch as there seems to be no reason for such displacements independent of the ordering.

It is not possible to determine unambiguously whether the three pyralspite components participate equally in the site exchange with Ca. One could speculate that crystal-field effects might favor Fe^{2+} as the key component, given that Mn^{2+}, Mg, and Ca do not experience crystal-field stabilization effects; using the mean O-*X*-O angles from Table 7 as ideal angles and applying a measure of distor-

tion analogous to octahedral angle variance (Robinson et al., 1971), the $X1$ site does turn out to be very slightly more distorted than the $X2$ site, which would presumably enhance the crystal-field stabilization energy of Fe^{2+} in $X1$ relative to $X2$ (see, for example, Burns, 1970, concerning the effects of polyhedral distortion on crystal-field stabilization energy). One could also argue that Ca ⇌ Mg cannot be the primary substitution because that would be inconsistent with the observed difference in electron densities of the two X sites.

In emphasizing the Landau approach to symmetry relationships, we have treated the ordering observed in the noncubic garnets discussed as if it arose by phase transition from a preexistent cubic phase with space group $Ia\bar{3}d$. Akizuki (1984) has argued that birefringence in grandites is a crystal-growth phenomenon that arises as ordering of Al and Fe^{3+} on different (110) growth steps occurs, making the steps crystallographically inequivalent, with each resulting growth sector having space group $I\bar{1}$. A treatment from a symmetry viewpoint based on the same group theoretical formalisms we have used here can also be applied to crystal growth, yielding the higher symmetry space groups that can result from superposition of triclinic growth sectors (Gali, 1983).

Hatch and Griffen (1989) argue that definitive evidence for discriminating between crystal growth and phase transition is lacking for the grandites. $MgSiO_3$ (Angel et al., 1988) and $MnSiO_3$ (Fujino et al., 1986) were both synthesized in high-pressure–high-temperature devices in experiments of short duration. Although the times required to bring the synthesized crystals to room conditions were not specified in either paper, it seems likely that they were quite short—perhaps too short to allow the nearly complete ordering of octahedral cations from an initially disordered state.

It would seem that the combination of high pressure (perhaps 0.8–1.2 GPa) and relatively low temperature (probably 200–400 °C) in the geologic environment in which garnet T-KAY-K-1 crystallized is the likely cause of the ordering. It is well known that increased pressure favors increased miscibility between pyralspites and grandites (e.g., Nemec, 1967), but it has been shown that heating of anisotropic grandites causes them to become optically isotropic (Hariya and Kimura, 1978; Allen and Buseck, 1988), that is, to become disordered. Garnets of compositions similar to ours but from geologic environments quite different from a paleosubduction zone have been described but have not been identified as birefringent (e.g., Sobolev et al., 1968), again suggesting that specific P,T conditions are important in determining whether a particular garnet chemically capable of ordering anisotropy will, in fact, order. Investigation of many more anisotropic garnets of various compositions and from differing geologic environments is required before more meaningful discussion on the influence on ordering of pressure, temperature, and composition can be undertaken.

Given an ordered garnet, the ordering route followed

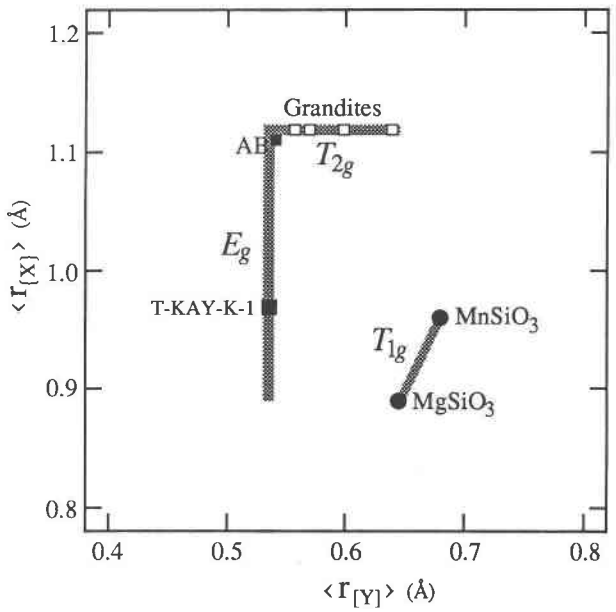

Fig. 3. Plot of mean cation sizes in the X and Y sites of noncubic garnets with structures refined to date. Gray bands indicate size ranges suggested by solid-solution series $Ca_3(Al,Fe^{3+})_2Si_3O_{12}$ (T_{2g}), $(Ca,Fe^{2+},Mg,Mn)_3Al_2Si_3O_{12}$ (E_g), and $(Mn,Fe^{2+},Mg)SiO_3$ (T_{1g}). AB indicates the garnet of Allen and Buseck (1988). $FeSiO_3$ garnet has not been synthesized, but it falls on the T_{1g} band and is likely a component of any tetragonal garnet that exists in the upper mantle.

(i.e., T_{2g}, T_{1g}, or E_g, regardless of whether ordering is considered to arise from a phase transformation or crystal growth) seems to depend primarily on the crystallographic sites potentially available for ordering and secondarily on the relative sizes of the cations in those sites. $MgSiO_3$, $MnSiO_3$, and the ordered grandites of Takéuchi et al. (1982) each contain a single type of cation in the X sites and two in the Y sites; this restricts potential ordering to the Y sites, with the T_{2g} route being followed if the Y cations are of similar size (e.g., Fe^{3+} and Al) and the T_{1g} route being followed if the Y cations are of very different sizes (e.g., Mn and Si). The grandite of Kingma and Downs (1989) evidently contains too little Mn in the X site for ordering to be detectable, if it occurs, so it too follows the T_{2g} route. Garnets that have two or more kinds of X cations in significant concentrations but only one significantly abundant kind of Y cation follow the E_g route; garnet T-KAY-K-1 is of this type.

These generalizations appear to apply when ordering is driven by a single order parameter, regardless of whether a phase transition or a primary growth phenomenon is assumed. They leave several important issues unaddressed, however. For example, only four of the eight space groups related to $Ia\bar{3}d$ by these IRs have been observed, and it is not at all clear what factors control the particular ordering pattern within a given ordering route; thus the specific factors that discriminate between the formation of an $I4_1/acd$ ordering pattern and an $Ibca$ or-

dering pattern are unknown. We have also not considered garnets that have the potential to order on more than one site; the near-grandite of Allen and Buseck (1988) is of this type, exhibiting ordering at both the X and Y sites. Figure 3 shows the mean radius of the Y cations plotted against that of the X cations for the noncubic garnets with structures refined thus far. The gray bands indicate size ranges predicted for the solid solution series $Ca_3(Al,Fe^{3+})_2Si_3O_{12}$ (T_{2g}), $(Fe^{2+},Mg,Mn)_3Al_2Si_3O_{12}$ (E_g), and $(Ca,Mn,Fe^{2+},Mg)SiO_3$ (T_{1g}). Investigation of the first issue—factors that determine the specific ordering pattern within an ordering route—will require examination of more noncubic garnets on the gray bands from as large a variety of geologic environments as possible. Investigation of the second issue—the nature of ordering driven by more than a single order parameter—will require examination of noncubic garnets that do not occur on the gray bands. The relative scarcity of such garnets does not minimize the fact that understanding them may shed light on processes ranging from the shallow crust to the upper mantle.

References cited

Akizuki, M. (1984) Origin of optical variations in grossular-andradite garnet. American Mineralogist, 69, 328–338.

Allen, F.M., and Buseck, P.R. (1988) XRD, FTIR, and TEM studies of optically anisotropic grossular garnets. American Mineralogist, 73, 568–584.

Angel, R.J., Finger, L.W., Hazen, R.M., Kanzaki, M., Weidner, D.J., Liebermann, R.C., and Veblen, D.R. (1989) Structure and twinning of single-crystal $MgSiO_3$ garnet synthesized at 17 GPa and 1800 °C. American Mineralogist, 74, 509–512.

Birman, J.L. (1966) Simplified theory of symmetry change in second-order phase transitions: Application to V_3Si. Physical Review Letters, 17, 1216–1219.

Burns, R.G. (1970) Mineralogical applications of crystal field theory. Cambridge University Press, Cambridge, England.

Cromer, D.T., and Liberman, D. (1970) Relativistic calculation of anomalous scattering factors for X-rays. Journal of Chemical Physics, 53, 1891–1898.

Cromer, D.T., and Mann, J.B. (1968) X-ray scattering factors computed from numerical Hartree-Fock wave functions. Acta Crystallographica, A24, 321–324.

Dempsey, M.J. (1980) Evidence for structural changes in garnet caused by calcium substitution. Contributions to Mineralogy and Petrology, 71, 281–282.

Dyar, M.D. (1984) Precision and interlaboratory reproducibility of measurements of the Mössbauer effect in minerals. American Mineralogist, 69, 1127–1144.

Fujino, K., Momoi, H., Sawamoto, H., and Kumazawa, M. (1986) Crystal structure and chemistry of $MnSiO_3$ tetragonal garnet. American Mineralogist, 71, 781–785.

Gali, S. (1983) Grandite garnet structures in connection with the growth mechanism. Zeitschrift für Kristallographie, 163, 43–52.

Geiger, C.A., Winkler, B., and Langer, K. (1989) Infrared spectra of synthetic almandine-grossular and almandine-pyrope garnet solid solutions: Evidence for equivalent site behaviour. Mineralogical Magazine, 53, 231–237.

Geller, S. (1967) Crystal chemistry of the garnets. Zeitschrift für Kristallographie, 125, 1–47.

Goldrich, F.E., and Birman, J.L. (1968) Theory of symmetry change in second-order phase transitions in perovskite structure. Physical Review, 167, 528–532.

Hahn, T., Ed. (1983) International tables for crystallography, vol. A. Reidel, Boston.

Hamilton, W.C. (1965) Significance tests on the crystallographic R factor. Acta Crystallographica, 18, 502–510.

Hariya, Y., and Kimura, M. (1978) Optical anomaly garnet and its stability field at high pressures and temperatures. Journal of the Faculty of Science, Hokkaido University, series IV, 18, 611–624.

Hatch, D.M. (1981a) Structural phase transitions in crystals of $R\bar{3}c$ symmetry. Physical Review, B23, 2346–2349.

——— (1981b) Order parameter symmetry for the β-γ transition in $Pb(VO_4)_2$. Physica Status Solidi, 106, 473–479.

Hatch, D.M., and Griffen, D.T. (1989) Phase transitions in the grandite garnets. American Mineralogist, 74, 151–159.

Hatch, D.M., and Stokes, H.T. (1985) Phase transitions in solids of diperiodic symmetry. Physical Review, B31, 4350–4354.

——— (1986) Systematic classification of symmetry changes in solid-solid phase transitions. In L.H. Bennett, Ed., Computer modeling of phase diagrams, p. 145–162. Metallurgical Society of AIME, Warrendale, Pennsylvania.

Hatch, D.M., Stokes, H.T., and Putnam, R.M. (1987) Symmetry analysis of the microstructure and phase transitions of a crystallographic space group: Applications. Physical Review, B35, 4935–4942.

Jaric, M.V., and Birman, J.L. (1977) Group theory of phase transitions in A-15 (O_h^3-$Pm3n$) structure. Physical Review, B16, 2564–2568.

Kingma, K.J., and Downs, J.W. (1989) Crystal-structure analysis of a birefringent andradite. American Mineralogist, 74, 1307–1316.

Kretz, R. (1983) Symbols for rock-forming minerals. American Mineralogist, 68, 277–279.

Kulaksiz, S., and Phillips, W.R. (1983) Mineralogy of a paleosubduction zone (Sivrigisar-Balçikhisar). Hacettepe Üniversitesi Yerbilimleri Uygulama ve Arastirma Merkezi Bülteni, 10, 95–104 (in Turkish).

Landau, L.D. (1937a) On the theory of phase transitions. I. Physikalische Zeitschrift der Sowjetunion, 11, 27–47 (in German).

——— (1937b) On the theory of phase transitions. II. Physikalische Zeitschrift der Sowjetunion, 11, 545–555 (in German).

Moore, R.K., White, W.B., and Long, T.V. (1971) Vibrational spectra of the common silicates: I. The garnets. American Mineralogist, 56, 54–71.

Nemec, D. (1967) The miscibility of the pyralspite and grandite molecules. Mineralogical Magazine, 37, 389–402.

North, A.C.T., Phillips, D.C., and Mathews, F.S. (1968) A semi-empirical method of absorption correction. Acta Crystallographica, A24, 351–359.

Novak, G.A., and Gibbs, G.V. (1971) The crystal chemistry of the silicate garnets. American Mineralogist, 56, 791–825.

Prewitt, C.T., and Sleight, A.W. (1969) Garnet-like structures of high-pressure cadmium germanate and calcium germanate. Science, 163, 386–387.

Rickwood, P.C. (1968) On recasting analyses of garnet into end-member molecules. Contributions to Mineralogy and Petrology, 18, 175–198.

Robinson, K., Gibbs, G.V., and Ribbe, P.H. (1971) Quadratic elongation: A quantitative measure of distortion in coordination polyhedra. Science, 172, 567–570.

Shannon, R.D. (1976) Revised effective ionic radii and systematic studies of interatomic distances in halides and chalcogenides. Acta Crystallographica, A32, 751–767.

Sheldrick, G.M. (1983) SHELXTL, An integrated system for solving, refining, and displaying crystal structures from diffraction data (4th revision). University of Göttingen, Göttingen, Germany.

Smyth, J.R., Madel, R.E., McCormick, T.C., Munoz, J.L., and Rossman, G.R. (1990) Crystal-structure refinement of a F-bearing spessartine garnet. American Mineralogist, 75, 314–318.

Sobolev, N.V., Jr., Kuznetsova, I.K., and Zyuzin, N.I. (1968) The petrology of grospydite xenoliths from the Zagodochnaya kimberlite pipe in Yakutia. Journal of Petrology, 9, 353–380.

Stokes, H.T., and Hatch, D.M. (1988) Isotropy subgroups of the 230 crystallographic space groups. World Scientific, Singapore.

Takéuchi, Y., Haga, N., Umizu, S., and Sato, G. (1982) The derivative structure of silicate garnets in grandite. Zeitschrift für Kristallographie, 158, 53–99.

Manuscript received February 5, 1991
Manuscript accepted November 1, 1991